Anomalous Nernst and Righi-Leduc Effects in Mn_3Sn: Berry Curvature and Entropy Flow

Xiaokang Li,[1] Liangcai Xu,[1] Linchao Ding,[1] Jinhua Wang,[1] Mingsong Shen,[1] Xiufang Lu,[1] Zengwei Zhu,[1,*] and Kamran Behnia[1,2,†]

[1]*Wuhan National High Magnetic Field Center and School of Physics, Huazhong University of Science and Technology, Wuhan 430074, China*

[2]*Laboratoire de Physique Et d'Etude des Matériaux (UPMC-CNRS), ESPCI Paris, PSL Research University, 75005 Paris, France*

(Received 19 December 2016; revised manuscript received 16 February 2017; published 1 August 2017)

We present a study of electric, thermal and thermoelectric response in noncollinear antiferromagnet Mn_3Sn, which hosts a large anomalous Hall effect (AHE). Berry curvature generates off-diagonal thermal (Righi-Leduc) and thermoelectric (Nernst) signals, which are detectable at room temperature and invertible with a small magnetic field. The thermal and electrical Hall conductivities respect the Wiedemann-Franz law, implying that the transverse currents induced by the Berry curvature are carried by Fermi surface quasiparticles. In contrast to conventional ferromagnets, the anomalous Lorenz number remains close to the Sommerfeld number over the whole temperature range of study, excluding any contribution by inelastic scattering and pointing to the Berry curvature as the unique source of AHE. The anomalous off-diagonal thermo-electric and Hall conductivities are strongly temperature dependent and their ratio is close to k_B/e.

DOI: 10.1103/PhysRevLett.119.056601

The ordinary Hall effect, the transverse electric field generated by a longitudinal charge current in the presence of a magnetic field, is caused by the Lorentz force exerted by a magnetic field on charge carriers. In ferromagnetic solids, there is an additional component to this response (known as extraordinary or anomalous) thought to arise as a result of a sizeable magnetization. During the past decade, a clear link between the anomalous Hall effect (AHE) and the Berry curvature of Bloch waves has been established [1,2]. Charged carriers of entropy are also affected by the Lorenz force. Therefore, one expects a transverse component to thermal conductivity called the Righi-Leduc (or the thermal Hall) effect [3] in the presence of a magnetic field. This is also the case of thermoelectric conductance, which acquires an off-diagonal component, α_{ij}, intimately linked to the Nernst coefficient, directly measurable by experiment [4]. When the Berry curvature replaces the magnetic field, counterparts of the AHE appear in the thermal and thermoelectric response of ferromagnets [5–8]. They can be an additional source of information regarding the fundamental mechanism leading to the generation of dissipationless transverse currents. Recently, following a proposition by Chen, Niu, and Macdonald [9], Nakatsutji *et al.* and Nayak *et al.* found a large AHE in Mn_3Sn [10] and Mn_3Ge [11,12], which are noncollinear antiferromagnets at room temperature. Several recent theoretical studies were devoted to this issue [13–15].

In this Letter, we present a study of the anomalous Righi-Leduc and Nernst effects (ANE) in Mn_3Sn in order to quantify the amplitude of these coefficients compared to their Hall counterpart. We detect a large anomalous Righi-Leduc conductivity and find that its magnitude corresponds to what is expected according to the Wiedemann-Franz (WF) law over an extended temperature window. The result confirms a theoretical prediction by Haldane [16] with important consequences for the debate regarding the two alternative formulations of anomalous Hall effect [16–18]. The AHE can be formulated as a property of the whole Fermi sea or the Fermi surface [16,18]. The expected magnitude of the anomalous Hall conductivity (AHC) in both pictures is identical (as explicitly shown in the case of bcc iron [19–21]). The verification of the Wiedemann-Franz law allows for an experimental distinction, since the validity of this law is straightforward in the Fermi-surface picture, but not necessarily in the Fermi-sea picture. We compare the robustness of the WF law in Mn_3Sn and in Fe and Ni-based ferromagnets [5] and find that inelastic scattering does not play any detectable role in generating the anomalous transverse coefficients of Mn_3Sn, in contrast to common ferromagnets. We also quantified the anomalous transverse thermoelectric response, α^A_{ij}, and argue that the magnitude and the temperature dependence of the ratio of α^A_{ij} to σ^A_{ij} is a source of information on the location of that Weyl nodes.

The Mn_3Sn single crystal was grown using the Bridgman-Stockbarger technique. Thermal and thermoelectric conductivity was measured with thermocouples (see [22] for details). The temperature dependence of the longitudinal transport coefficients are shown in Fig. 1. As seen in the figure, resistivity attains a magnitude of 250 $\mu\Omega$ cm and becomes almost flat at room temperature. Electric and thermal conductivities are both almost isotropic, in contrast to the Seebeck coefficient. The temperature dependence of magnetization, measured in field-cooled (FC) conditions, is similar to what was previously reported [26]. It shows that the system becomes magnetically ordered below $T_N = 420$ K and above $T_1 = 200$ K with a weak ferromagnetic remanence. Tomiyoshi and Yamauguchi [27] studied the magnetic texture of this system by polarized neutron diffraction decades ago and, following an earlier study [28], suggested a triangular spin structure stabilized by the Dzyaloshinski-Moriya interaction [Fig. 1(e)]. An alternative magnetic texture [Fig. 1(f)] will be considered below in light of a recent theoretical calculation [14].

Two points are to be noticed about transport of charge and entropy in this metal. First, given the carrier density ($n = 2 \times 10^{22}$ cm^{-3} [10,22]), a room-temperature resistivity of 250 $\mu\Omega$ cm implies a mean-free-path as short as 0.7 nm. This is comparable to the lattice parameters ($a = 0.566$ nm and $c = 0.453$ nm [27]). Thus, the system is close to the Mott-Ioffe-Regel limit, and the saturation of resistivity between 300 and 400 K is not surprising [29]. Second, the room-temperature Lorenz number ($L_{ii} = [\kappa_{ii}(300\ \mathrm{K})\rho_{ii}(300\ \mathrm{K})/300\ \mathrm{K}]$) is almost twice the Sommerfeld number, $L_0 = 2.44 \times 10^{-8} V^2 K^{-2}$. Therefore, the total contribution of phonons and magnons to the longitudinal thermal transport is comparable to the electronic heat transport.

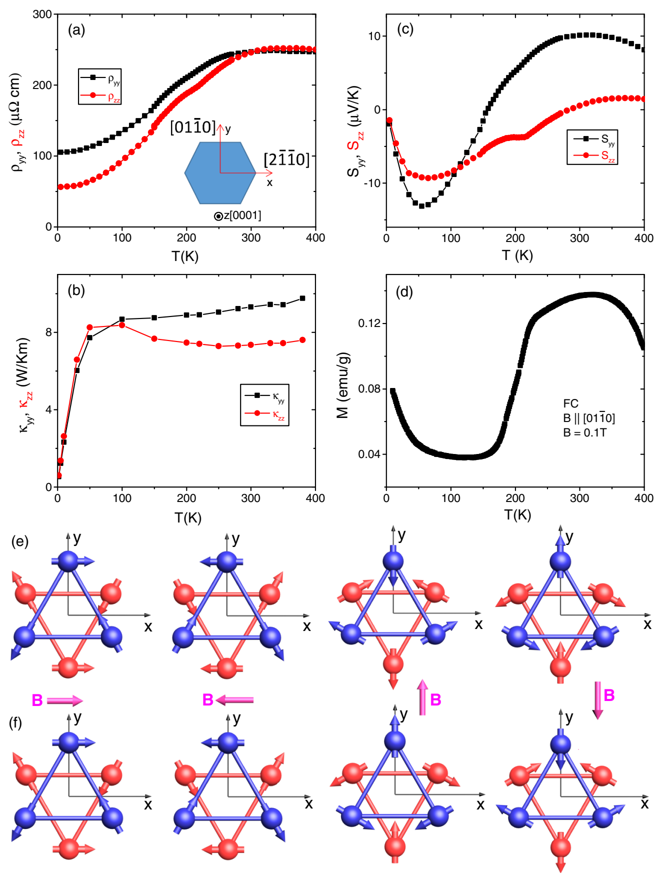

FIG. 1. Zero-field temperature dependence of resistivity (a), thermal conductivity (b), Seebeck coefficient (c), and the field cooled (FC) magnetization (d). Panels (e) and (f) show magnetic texture for four different orientations of magnetic field. Blue and red circles represent Mn atoms in adjacent planes. Panel (e) is the set of configurations proposed in Ref. [27]. Panel (f) starts with the chirality considered in a theoretical calculation [14] and assumes that the spins rotate freely with the magnetic field. In (e), Mn spins, which are parallel to the field when $B \| x$, become antiparallel when $B \| y$. In (f), the magnetic field and the spins keep their mutual orientations.

What makes this magnetic metal remarkable is its transverse transport, illustrated in Fig. 2. With a current along [0001] (dubbed the z axis) and a magnetic field along [01$\bar{1}$0] (dubbed the y axis), there is a large and hysteretic jump in the Hall resistivity, ρ_{xz}. Its magnitude (7.6 $\mu\Omega$ cm) is comparable to what was reported previously [10] and is reversible with a field as small as 0.1 T. The Nernst coefficient [Fig. 2(c)] shows a jump of 1 μV/K, a remarkably large value. Given the low mobility ($\sim$1.7 cm$^2 V^{-1} s^{-1}$) and the large Fermi energy ($\sim$2.6 eV) of the system, this is 6 orders of magnitude larger than the expected quasiparticle response [4]. The same setup was used to measure the AHE and ANE of an iron single crystal to obtain data similar to what was previously reported [24,25]. They are presented in Fig. S1 of the Supplemental Material [22]. In Mn_3Sn, the

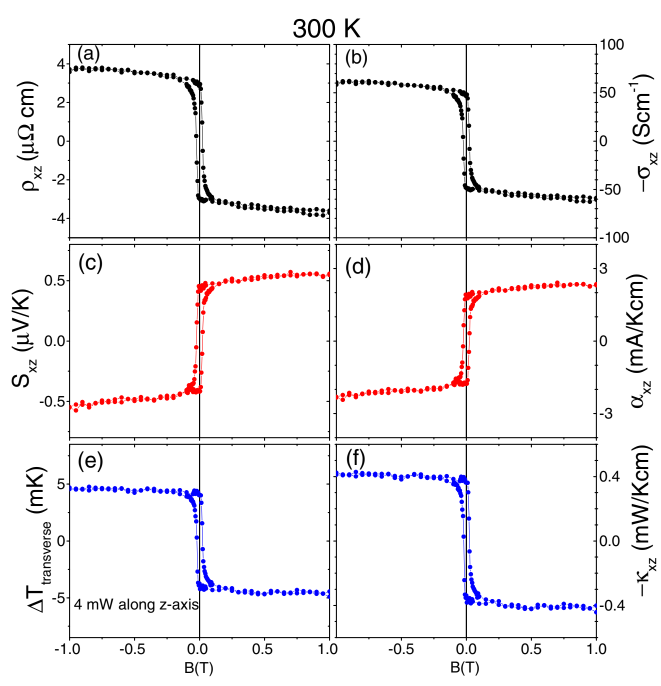

FIG. 2. Room-temperature field dependence of transport coefficients with magnetic field is applied along the y axis ([01$\bar{1}$0]) and the charge or heat current along the z axis ([0001]). (a) Hall resistivity, ρ_{xz}); (b) Hall conductivity, σ_{xz}, extracted from ρ_{xz}, ρ_{xx}, and ρ_{zz}; (c) Nernst signal, S_{xz}; (d) Transverse thermoelectric conductivity, α_{xz}, extracted from S_{xz}, S_{zz}, ρ_{xx}, ρ_{zz}, and ρ_{xz}; (e) The transverse thermal gradient generated by a longitudinal heat current along the z axis. (f) The extracted Righi-Leduc coefficient, κ_{xz}.

anomalous transport coefficients dominate their ordinary counterparts, leading to a steplike profile quite distinct from what is seen in ferromagnets such as iron [24,25] or cobalt [30].

From Hall resistivity, ρ_{xz} and Nernst response, S_{xz}, one can extract the magnitude of Hall conductivity, σ_{xz} [Fig. 2(b)], and transverse thermoelectric conductivity, α_{xz} [Fig. 2(d)]. This can be done by manipulating $\bar{\rho}$, $\bar{\sigma}$, $\bar{\alpha}$, and $\bar{S}$ tensors (See the Supplemental Material [22]). We also found a purely thermal counterpart to anomalous electric and thermoelectric responses. As seen in Fig. 2(e), applying a thermal current along the z axis generates a transverse thermal gradient along the x axis, which can be inverted by a magnetic field applied along the y axis. This allows us to extract the amplitude of thermal Hall (Righi-Leduc) conductivity, κ_{xz} [Fig. 2(f)].

The anomalous electric and thermoelectric transport coefficients were studied at different temperatures in two configurations ($B//y$ and $B//x$). Figure 3 presents the field dependence of σ_{xz}, σ_{zy}, α_{xz}, and α_{zy} at several temperatures. As seen in the figure, the behavior remains steplike down to 200 K and the magnitude of all coefficients smoothly increases with decreasing temperature. At $T_1 \simeq 200$ K, the triangular spin order is destroyed [31–33] and all anomalous transport coefficients disappear below this temperature as seen in the bottom panels of Fig. 3, which present the temperature dependence of σ^A_{ij} and α^A_{ij}. This confirms that the remarkably large magnitude of zero-field transverse transport coefficients is a property of the non-collinear antiferromagnet stabilized between 420 and 200 K. This phase transition to what seems to be a glassy ferromagnetic order [33,34] at 200 K is specific to Mn_3Sn and does not occur in its sibling Mn_3Ge [11,12]. In the following, we will focus on the magnitude of the anomalous transport coefficients in the magnetic phase hosting the triangular spin order. Two correlations are relevant here. The first is the Wiedemann-Franz law

$$L^A_{ij} = \frac{\kappa^A_{ij}}{T\sigma^A_{ij}} = L_0 = \frac{\pi^2}{3}\left(\frac{k_B}{e}\right)^2. \tag{1}$$

The second is the Mott formula

$$\alpha_{ij} = -\frac{\pi^2}{3}\frac{k_B}{e}k_B T\frac{\partial\sigma_{ij}}{\partial E}\bigg|_{E_F}. \tag{2}$$

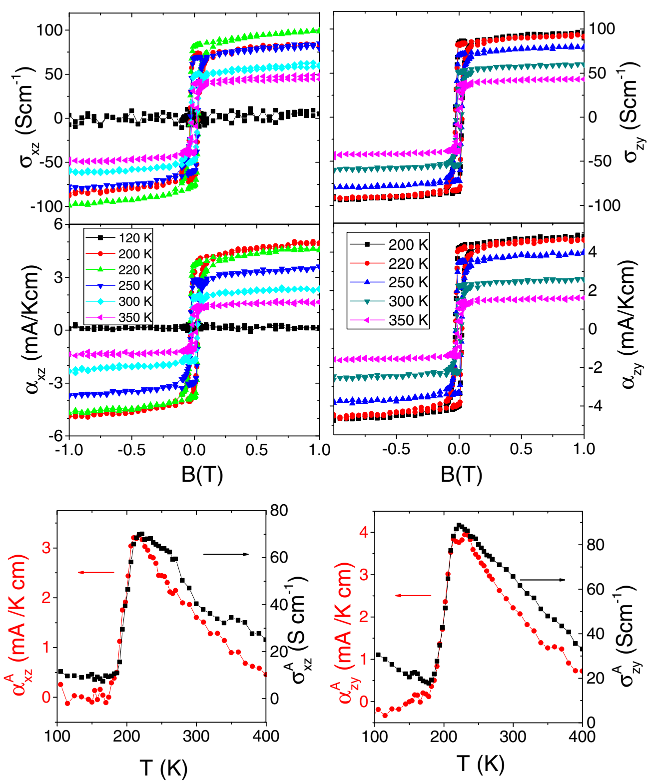

FIG. 3. Top: Field dependence of σ_{xz} and α_{xz} (left) and σ_{zy} and α_{zy} (right) at different temperatures. Bottom: The temperature dependence of σ^A_{xz} and α^A_{xz} (left) and σ^A_{zy} and α^A_{zy} (right). Note the phase transition at $T^* \sim 200$ K leading to the collapse of all anomalous transport coefficients. For both orientations, α^A_{ij} raises faster than σ^A_{ij}.

Figure 4 presents the field dependence of κ_{xz} and κ_{zy} at different temperatures and the temperature dependence of the anomalous Lorenz number, $L^A_{ij} = \kappa^A_{ij}/T\sigma^A_{ij}$. As one can see in the bottom panels of Fig. 4, in the temperature range of triangular spin order (i.e., from 400 down to 200 K), the experimentally resolved L^A_{ij} remains close to L_0. Thus, the anomalous thermal and electrical Hall conductivities obey the correlation dictated by the Wiedemann-Franz law.

The intrinsic AHE arises as a result of an additional term in the group velocity of Bloch electrons [35]

$$\dot{r} = \frac{1}{\hbar}\frac{\partial\epsilon_{n(\mathbf{k})}}{\partial\mathbf{k}} + \dot{\mathbf{k}} \times \Omega_n(\mathbf{k}). \tag{3}$$

Here, $\Omega_n(\mathbf{k})$ is the local Berry curvature. In the presence of an electric field, E, $\dot{\mathbf{k}} = -eE/\hbar$. Starting from this, an expression for σ^A_{ij} in the presence of the Berry curvature, Ω^k_n (n is a band index) has been driven [1,2,8]

$$\sigma^A_{ij} = \frac{-e^2}{\hbar}\sum_n \int_{\mathrm{BZ}} \frac{d^3k}{(2\pi)^3} f_n(k)\Omega^k_n(k). \tag{4}$$

The expression is similar to the topological formulation of the Quantum Hall effect [36]. Note that the integral is taken over the whole Brillouin zone (BZ). Haldane [16] noticed that in such an expression, the AHE appears as a property of the whole Fermi sea and not the Fermi surface, but this would contradict the sprit of Landau's Fermi liquid theory. He showed that an alternative expression for AHE is [16,18]

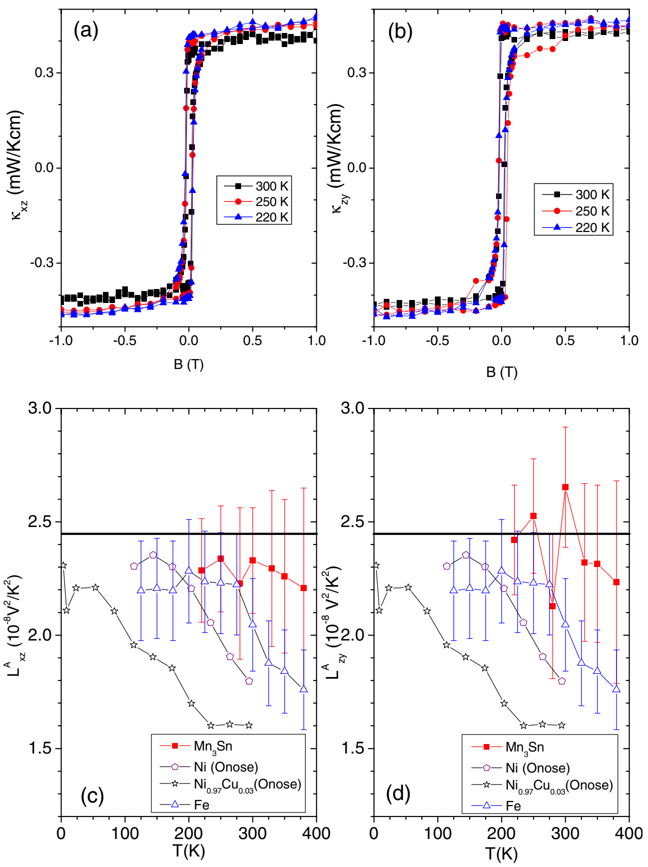

FIG. 4. Top: The field dependence of κ_{xz} (a) and κ_{zy} (b) at different temperatures (More data at other temperatures are in the Supplemental Material [22]). Bottom: The temperature dependence of anomalous Lorenz number L^A_{xz} (c) and L^A_{zy} (d). The anomalous Lorenz number of Ni [5], $Ni_{0.97}Cu_{0.03}$ [5], and Fe [22] are also shown. Error bars are large, because the thermal and electrical measurements were performed with different contacts. Solid horizontal lines represent L_0.

$$\sigma^A_{ij} = \frac{-e^2}{\hbar}\sum_n \int_{S_n} \frac{d^2k}{(2\pi)^2}[\Omega^k_n(k).\hat{n}(k)]\mathbf{k}. \tag{5}$$

Here, the integral is taken over the Fermi surface S_n of band n, and $\hat{n}(k)$ is the unit vector perpendicular to the surface. The two formulations were recognized as equivalent [1] and yield quasi-identical values of σ^A_{xy} in iron ($\sim$750 S cm^{-1}) [19,20], close to the room-temperature experimental value ($\sim$1000 S cm^{-1} [22,24]).

Let us consider what the existence of κ^A_{ij} implies. If the electronic states in question possess an entropy, S_k, a temperature gradient generates a force, and $\dot{\mathbf{k}} = -S_k\nabla T/\hbar$. Now, in a Fermi-Dirac distribution, the interface between occupied and unoccupied states is the only reservoir of entropy [37]. In other words, only states at the Fermi surface (and not those deep inside the Fermi sea) can feel a force exerted by a temperature gradient. The validity of the Wiedemann-Franz law implies that the transverse electronic flow generated by the Berry curvature is a flow of charge and entropy with a ratio of $(\pi^2/3)(k_B/e)^2$. This rules out any contribution to σ^A_{ij} by Weyl nodes of the entirely occupied bands, the central issue in the Fermi-sea vs Fermi-surface debate [17,18].

Previous to this study, Onose *et al.* [5] measured the anomalous thermal Hall conductivity of ferromagnetic Ni and $Ni_{0.97}Cu_{0.03}$ and found that the Wiedemann-Franz law is satisfied at low temperatures. We performed similar measurements on an Fe single crystal [22] and found similar results. The lower panels of Fig. 4 compare all sets of data. One can see that, in common ferromagnets, L^A_{ij} is close to L_0 in the zero-temperature limit and a steady downward trend is visible at a finite temperature. Now, the Wiedemann-Franz law is only valid in the absence of inelastic scattering [38]. The Lorenz-Sommerfeld ratio is expected to deviate downward from unity in the presence of inelastic scattering. Such a deviation is clearly present in the Ni and $Ni_{0.97}Cu_{0.03}$ [5] as well as Fe, but undetectable in Mn_3Sn. This implies that inelastic scattering plays a role in generating the room-temperature anomalous transverse response in the ferromagnets but not in Mn_3Sn. Therefore, one can exclude not only a phonon contribution [39], but also skew scattering by magnons as a partial source of AHE in Mn_3Sn. Therefore, our study identifies the robustness of the WF law as a means to distinguish between distinct sources of AHE [1].

The peak magnitude of AHC found in this study ($\sigma^A_{xz} \simeq$ 70 S cm^{-1} $\sigma^A_{zy} \simeq 90$ S cm^{-1} at 200 K) is close to what was reported previously [10]. First principle theory has shown that the expected magnitude of AHC strongly depends on the chirality of the spin texture [13]. According to a recent theoretical study [14], for the spin texture shown in Fig. 1(f), $\sigma^A_{xz} = 133$ S cm^{-1} and $\sigma^A_{zy} = 0$. However, if the spin structure rotates easily with the magnetic field, then one expects comparable magnitudes for the two configurations in agreement with experimental observation. Since σ^A_{xz} and σ^A_{zy} keep the sign of their normal counterparts, the chirality is expected to be identical for the two configurations [Fig. 1(f)] in contrast to the configuration scheme proposed by early studies of polarized neutron diffraction [Fig. 1(e)].

Thus, the theoretically expected and the experimentally observed AHC are close to each other, but the strong temperature dependence raises a fundamental question. Low-field ordinary Hall conductivity is proportional to the square of the mean free path [4,40]. On the other hand, topological Hall conductivity, like in the quantum Hall effect [36], does not depend on the mean free path. If the AHE is a topological property of the electronic system and independent of the carrier mean free path, why does its magnitude decrease by a factor of 3 when the system is warmed from 200 to 400 K? There is no trace of such a strong variation in iron [22]. The magnitude and the temperature dependence of ANE brings additional insight. Ordinary Nernst response roughly scales with k_BT/E_F [4].

Here, with cooling, α_{ij}^A rises faster than σ_{ij}^A (See Fig. 3). The $\alpha_{ij}^A/\sigma_{ij}^A$ ratio evolves from 15 μV/K at room temperature to 50 μV/K around 220 K. This is a sizeable fraction of $k_B/e = 86$ μV/K and, unlike its ordinary counterpart, is not attenuated by k_BT/E_F. An $\alpha_{ij}^A/\sigma_{ij}^A$ ratio close to k_B/e appears to confirm the purely topological origin of AHE. The temperature dependence may be due to a temperature-induced shift in the locus of Weyl nodes.

In summary, we quantified the anomalous transverse response of Mn_3Sn. The Wiedemann-Franz law is robust with no sign of downward deviation, excluding any contribution from inelastic scattering. This implies that (i) the electrical Hall current has a purely thermal counterpart carried by Fermi surface quasiparticles, and (ii) in Mn_3Sn, in contrast to common ferromagnets, inelastic scattering does not play any role in generating the AHE response, pointing to a purely topological origin.

We acknowledge useful discussions with M. O. Goerbig. Z. Z. was supported by the 1000 Youth Talents Plan and the work was supported by the National Science Foundation of China (Grant No. 11574097) and The National Key Research and Development Program of China (Grant No. 2016YFA0401704). K. B. was supported by China High-End Foreign Expert Programme, the 111 Project (B13033) and Fonds-ESPCI-Paris.

*zengwei.zhu@hust.edu.cn
†kamran.behnia@espci.fr

[1] N. Nagaosa, J. Sinova, S. Onoda, A. H. MacDonald, and N. P. Ong, Rev. Mod. Phys. **82**, 1539 (2010).
[2] D. Xiao, M.-C. Chang, and Q. Niu, Rev. Mod. Phys. **82**, 1959 (2010).
[3] Y. Zhang, N. P. Ong, Z. A. Xu, K. Krishana, R. Gagnon, and L. Taillefer, Phys. Rev. Lett. **84**, 2219 (2000).
[4] K. Behnia and H. Aubin, Rep. Prog. Phys. **79**, 046502 (2016).
[5] Y. Onose, Y. Shiomi, and Y. Tokura, Phys. Rev. Lett. **100**, 016601 (2008).
[6] W.-L. Lee, S. Watauchi, V. L. Miller, R. J. Cava, and N. P. Ong, Phys. Rev. Lett. **93**, 226601 (2004).
[7] T. Miyasato, N. Abe, T. Fujii, A. Asamitsu, S. Onoda, Y. Onose, N. Nagaosa, and Y. Tokura, Phys. Rev. Lett. **99**, 086602 (2007).
[8] D. Xiao, Y. Yao, Z. Fang, and Q. Niu, Phys. Rev. Lett. **97**, 026603 (2006).
[9] H. Chen, Q. Niu, and A. H. MacDonald, Phys. Rev. Lett. **112**, 017205 (2014).
[10] S. Nakatsuji, N. Kiyohara, and T. Higo, Nature (London) **527**, 212 (2015).
[11] A. K. Nayak *et al.*, Sci. Adv. **2**, e1501870 (2016).
[12] N. Kiyohara, T. Tomita, and S. Nakatsuji, Phys. Rev. Applied **5**, 064009 (2016).
[13] J. Kübler and C. Felser, Europhys. Lett. **108**, 67001 (2014).
[14] H. Yang, Y. Sun, Y. Zhang, W.-J. Shi, S. S. P. Parkin, and B. Yan, New J. Phys. **19**, 015008 (2017); Y. Zhang, Y. Sun, H. Yang, J. Zelezny, S. P. P. Parkin, C. Felser, and B. Yan, Phys. Rev. B **95**, 075128 (2017).
[15] M.-T. Suzuki, T. Koretsune, M. Ochi, and R. Arita, Phys. Rev. B **95**, 094406 (2017).
[16] F. D. M. Haldane, Phys. Rev. Lett. **93**, 206602 (2004).
[17] Y. Chen, D. L. Bergman, and A. A. Burkov, Phys. Rev. B **88**, 125110 (2013).
[18] D. Vanderbilt, I. Souza, and F. D. M. Haldane, Phys. Rev. B **89**, 117101 (2014).
[19] D. Gosálbez-Martínez, I. Souza, and D. Vanderbilt, Phys. Rev. B **92**, 085138 (2015).
[20] Y. Yao, L. Kleinman, A. H. MacDonald, J. Sinova, T. Jungwirth, D. S. Wang, E. Wang, and Q. Niu, Phys. Rev. Lett. **92**, 037204 (2004).
[21] X. Wang, J. R. Yates, I. Souza, and D. Vanderbilt, Phys. Rev. B **74**, 195118 (2006).
[22] See Supplemental Material at http://link.aps.org/supplemental/10.1103/PhysRevLett.119.056601 for more detailed experimental methods, the raw data in iron, the raw data on field dependence of the transverse thermal and electric conductivities of Mn_3Sn, and the derivations of off-diagonal components of the transport tensors, which includes Refs. [10, 19–21, 23–25].
[23] Y. Shiomi, Y. Onose, and Y. Tokura, Phys. Rev. B **81**, 054414 (2010).
[24] P. N. Dheer, Phys. Rev. **156**, 637 (1967).
[25] S. J. Watzman, R. A. Duine, Y. Tserkovnyak, S. R. Boona, H. Jin, A. Prakash, Y. Zheng, and J. P. Heremans, Phys. Rev. B **94**, 144407 (2016).
[26] H. Ohmori, S. Tomiyoshi, H. Yamauchi, and H. Yamamoto, J. Magn. Magn. Mater. **70**, 249 (1987).
[27] S. Tomiyoshi, J. Phys. Soc. Jpn. **51**, 803 (1982); S. Tomiyoshi and Y. Yamaguchi, J. Phys. Soc. Jpn. **51**, 2478 (1982).
[28] G. J. Zimmer and E. Krén, AIP Conf. Proc. **10**, 1379 (1973).
[29] O. Gunnarsson, M. Calandra, and J. E. Han, Rev. Mod. Phys. **75**, 1085 (2003).
[30] J. Kötzler and W. Gil, Phys. Rev. B **72**, 060412(R) (2005).
[31] E. Krén, J. Paitz, G. Zimmer, and É. Zsoldos, Physica (Amsterdam) **80**, 226 (1975).
[32] S. Tomiyoshi, S. Abe, Y. Yamaguchi, H. Yamauchi, and H. Yamamoto, J. Magn. Magn. Mater. **54–57**, 1001 (1986).
[33] P. J. Brown, V. Nunez, F. Tasset, J. B. Forsyth, and P. Radhakrishna, J. Phys. Condens. Matter **2**, 9409 (1990).
[34] W. J. Feng, D. Li, W. J. Ren, Y. B. Li, W. F. Li, J. Li, Y. Q. Zhang, and Z. D. Zhang, Phys. Rev. B **73**, 205105 (2006).
[35] M.-C. Chang and Q. Niu, Phys. Rev. B **53**, 7010 (1996).
[36] M. Kohmoto, Ann. Phys. (N.Y.) **160**, 343 (1985).
[37] K. Behnia, *Fundamentals of Thermoelectricity* (Oxford University Press, New York, 2015).
[38] J. Ziman, *Principles of the Theory of Solids* (Cambridge University Press, Cambridge, England, 1972).
[39] C. Strohm, G. L. J. A. Rikken, and P. Wyder, Phys. Rev. Lett. **95**, 155901 (2005).
[40] N. P. Ong, Phys. Rev. B **43**, 193 (1991).